Nonisothermal Crystallization Kinetics of Flame-Sprayed Polyamide 1010/nano-ZrO_2 Composite Coatings

Ya-Dong Li,[1] Yi-Zhu Ma,[1] Fu-Feng Yan,[1] Shao-Kui Cao[2]

[1]*Department of Material Engineering, Zhengzhou Institute of Light Industry, Zhengzhou 450002, China*
[2]*College of Materials Engineering, Zhengzhou University, Zhengzhou 450052, China*

Received 8 January 2007; accepted 10 April 2007
DOI 10.1002/app.26802
Published online 16 July 2007 in Wiley InterScience (www.interscience.wiley.com).

ABSTRACT: Polyamide1010 (PA1010) and its composite with nanometer-sized zirconia (PA1010/nano-ZrO_2) coatings were deposited using a flame spray process. The kinetics of nonisothermal crystallization of PA1010/nano-ZrO_2 composite coatings was investigated by differential scanning calorimetry (DSC) at various cooling rates. Several different analysis methods were used to describe the process of nonisothermal crystallization. The results showed that the modified Avrami equation and Mo's treatment could describe the nonisothermal crystallization of the composite coatings very well. The nano-ZrO_2 particles have a remarkable heterogeneous nucleation effect in the PA1010 matrix. The values of halftime and Z_c showed that the crystallization rate increased with increasing cooling rates for both PA1010 and PA1010/nano-ZrO_2 composite coating, but the crystallization rate of PA1010/nano-ZrO_2 composite coating was faster than that of PA1010 at given cooling rate. © 2007 Wiley Periodicals, Inc. J Appl Polym Sci 106: 1535–1543, 2007

Key words: flame-sprayed; polyamide1010; nano-ZrO_2; composite coating

INTRODUCTION

Thermal spray is an excellent solution for overcoming the processing limitations of other coating application techniques. Thermal spraying processes use in combustion or an electric arc as a heat source to melt materials that can be produced in the form of powder, wire or rods. The molten particles produced during the spraying are accumulate to form a coating. In consequently, Thermal-sprayed surfaces are now broadly used in industrial applications to improve surface protection against corrosion and wear.[1–8]

Poly(iminosebacoyl iminodecamethylene), (PA1010), which is an extraordinary semicrystalline polyamide, is especially manufactured commercially in China. Besides of the common features, it has a notable resistance to moisture when compared with polyamide 6, 6 as well. Mo et al. reported the crystalline structure and thermodynamic parameters of PA1010, PA1010 crystallization in the triclinic system, with the following lattice dimensions: $a = 0.49$ nm, $b = 0.54$ nm, $c = 2.78$ nm, $\alpha = 49^\circ$, $\beta = 77^\circ$, $\gamma = 63.5^\circ$.[9]

Correspondence to: Y.-D. Li (lyd8@zzuli.edu.cn).
Contract grant sponsor: University Prominent Research Talents; contract grant number: 2006KYCX007.

It is well understood that the physical, chemical and mechanical properties of crystalline and semicrystalline polymers depend on the morphology, the crystalline phase and degree of crystallization. Moreover, the change of crystallization behavior can further influence the properties of final product. To control the rate of the crystallization and the degree of crystallinity to obtain the desired morphology and properties, a great deal of effort has been done for studying the crystallization kinetics and the corresponding material properties.[10–12] Research for the polymer crystallization process can be carried out under isothermal or nonisothermal conditions. Analysis of overall crystallization rate under isothermal conditions is generally accomplished by use of Avrami equation, which is valid at least for the early stages of the process. Although the treatment of nonisothermal crystallization is more complex, yet for its study is of great interest, because its conditions are closer to real industrial processing conditions. While there have been a few papers[13,14] dealing with the crystallization behavior of PA1010 and PA1010/nanoparticles composites, little work has been done on flame sprayed PA1010 composite coatings.

In the present work, the crystallization behavior of PA1010/nano-ZrO_2 composite coating was investigated under nonisothermal conditions. Three nonisothermal crystallization kinetics equations were used for the analysis.

EXPERIMENTAL

Materials

Nano-ZrO_2 which supplied by Laboratory of Special Functional Materials of Henan University, Henan, China was used as additional reinforcement. Figure 1 is the TEM images of the ZrO_2 nanoparticles, which shows that the quasi-spherical particles are well separated and almost monodisperse. The average size of particles is about 4 nm in diameter. Figure 2 displays the XRD pattern of the sample of ZrO_2 powders. According to standard ZrO_2 (JCPDS: 79-1770), the stronger peak at 30.9° is assigned to (101) crystalline plane of ZrO_2 and the sample has a stable tetragonal structure. Furthermore, diffractions of sample at 49.8° and 60.3° may overlap each other for the very small sizes of nanoparticles.

The PA1010 powders were purchased from Shanghai Celluloid Factory, China. Its size is less than 200 μm. To vary the interaction of the polymer with the zirconia particles, the zirconia surface was modified chemically. Co-spraying two powders could result in significant powder segregation in the jet due to the differences in powder size and density. Powders were preconditioned for spraying by ultrasonic mixing PA1010 together with the nano-particulate phase for 2 h to produce a composite powder. The composite powder was dried in vacuum oven before thermal spraying at 80°C for 24 h to remove excess moisture. The composite powder aids both in distributions of the filler in the coating and in simultaneous powder feeding into the flame spray jet.

Flame spray

Nanocomposite coatings containing 0.5, 1.0, 1.5, 2.0, and 2.5 wt% ZrO_2 nanoparticles were prepared in thermal-spraying over 45# steel substrate with the plastic flame spray system. Acetylene and compressed air were used to produce the combustion flame. Here, compressed air was used to fluidize the powder mixture, and transport the powder blend from the fluidized bed to the torch, where it was added to the combustion gas for generation of the flame. The substrates were grit blasted immediately before thermal spraying. In the process of spraying, optimal compressed air pressure, acetylene pressure, powder carrier gas pressure and spray distance have been evaluated previously,[15] and were kept constant at these values summarized in Table I. Meanwhile, the substrates were preheated to ~ 80°C by traversing the flame jet over the substrate surface before powder injection. Typical coating thickness was fixed at approximately 0.8 ~ 1.0 mm. Afterwards, the cooling of the coating was carried out in air at room temperature.

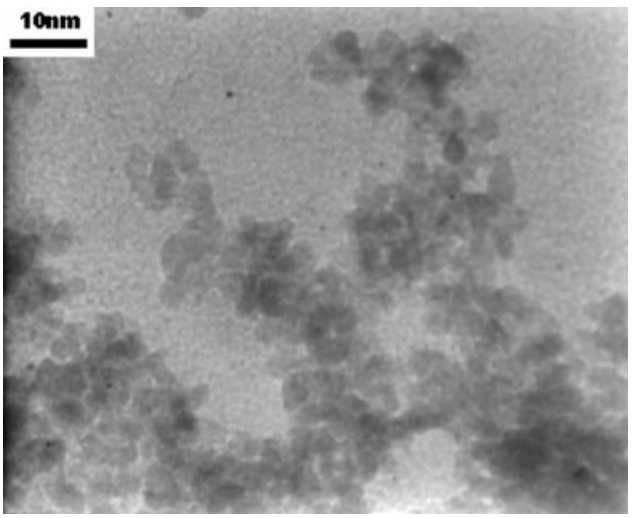

Figure 1 TEM image of ZrO_2 nanopaticles.

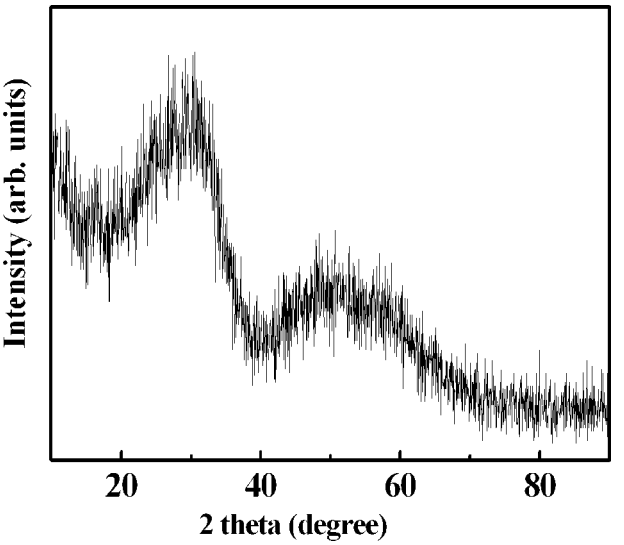

Figure 2 XRD pattern of ZrO_2 nanopaticles.

XRD and TEM analysis

The average size of the ZrO_2 particles was determined by transmission electron microscopy (TEM) with a JEM-200CXII (JEOL) microscope at 200 kV. Crystals of ZrO_2 particles were examined by X-ray diffraction (XRD) using a X′ Pert Pro MPD diffrac-

TABLE I
Plastic Flame Spray Parameters

Item	Parameter	
Compressed air pressure	0.6	1.2 MPa
Acetylene pressure	0.1	0.2 MPa
Powder carrier gas pressure	0.4	0.6 MPa
Spray distance	0.50	0.75 mm

tometer operated at 40 kV and 40 mA with Cu-Kα (λ = 1.54056 Å). The mean crystallite sizes of the ZrO_2 powders were determined by the XRD–Scherrer formula (mean crystallite size = 0.9λ/(β cos θ), where β is the half width of the diffraction peak and θ is the Bragg angle).

Differential scanning calorimetry analysis

The nonisothermal analyses were carried out using a TA Q100 differential scanning calorimeter thermal analyzer. All differential scanning calorimetry (DSC) measurements were performed under a nitrogen atmosphere on samples of round sheet of 4 ~ 6 mg. The samples were heated from 20 to 250°C at a heating rate of 20°C/min and kept at 250°C for 5 min to eliminate thermal history, and then cooled to 20°C at a cooling rate of 2.5, 5, 10, 15, 20°C/min, respectively. The thermograms corresponding to the cooling curves were recorded and analyzed to estimate the nonisothermal crystallization kinetics and crystallinity degree.

RESULTS AND DISCUSSION

Nonisothermal crystallization behavior

Figure 3 shows the curves of the heat flow as a function of the temperature during the nonisothermal crystallization of PA1010 and its nanocomposite coating at different cooling rates, respectively. As the cooling rate increased from 2.5 to 20 °C/min, the exothermic peak temperature decreased from 181.7 to 173.0°C, and the exotherms became border. As seen from Figure 3, the crystallization peak shifts to lower temperature with an increase in cooling rate for both pure PA1010 and PA1010/nano-ZrO_2 composite coating. Consequently, crystallization occurred at lower temperatures with fast cooling rates. The motion of PA1010 molecules cannot follow the cooling temperature when the cooling rate becomes faster. From these curves, the values of T_p (crystallization peak temperature), T_i (initial crystallization temperature), Δw (half-width of crystallization peak), and ΔH_c (the crystallization enthalpy) of PA1010 and its composite coatings could be determined. Moreover, X_c (the degree of crystallinity) can be calculated from the heat evolved during crystallization (ΔH_c) with the following relation to:

$$X_c(\%) = \frac{\Delta H_c}{[(1-\lambda)\Delta H_m]} \quad (1)$$

where ΔH_m = 244 J/g is the heat of fusion for 100% crystalline PA1010 and λ is the weight fraction of the filler in the composites. The values of X_c, T_i, T_p, Δw, ΔH_c, of PA1010/nano-ZrO_2 composite coatings with varying zirconia levels are listed in Table II. T_i, T_p, and X_c of the nanocomposite coatings are higher than those of PA1010 and ΔW of the PA1010/nano-ZrO_2 composite coating is smaller than that of PA1010 coating at the same crystallization conditions. It indicates that the addition of nano-ZrO_2 into PA1010 results in an increase of the degree of crystallinity and the peak crystallization temperature at various cooling rates. It can be explained that PA1010 segments could be absorbed on the surface of nano-ZrO_2 because of the large specific surface area and hydroxyl groups of the modifier on the surface of nano-ZrO_2.

Nonisothermal crystallization kinetics

As for the non-isothermal crystallization kinetics of nanocomposites, the relative degree of crystallinity

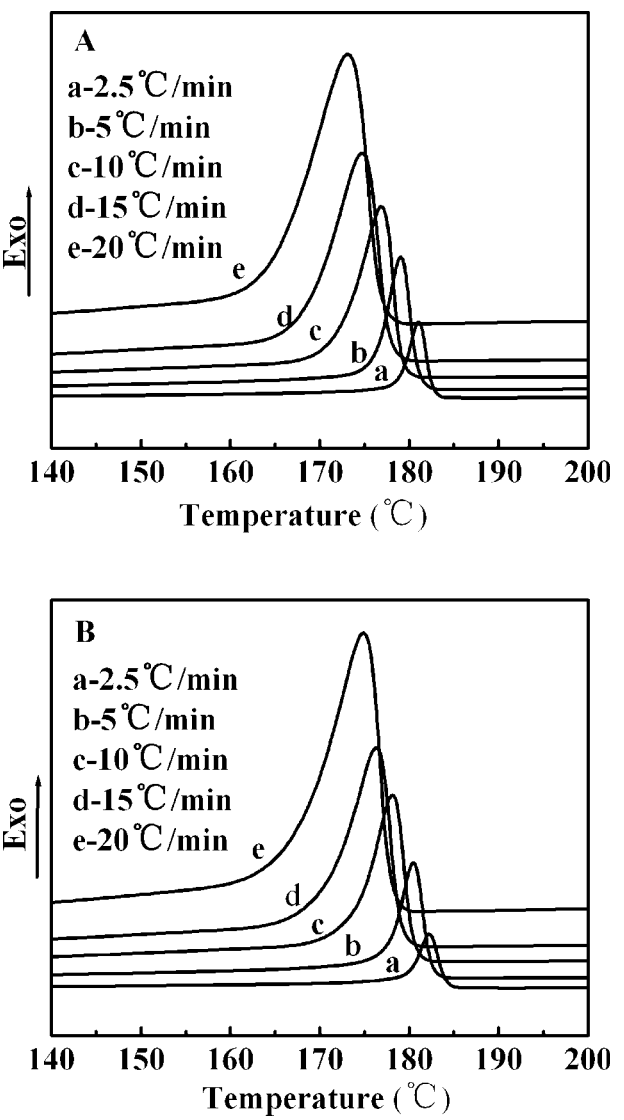

Figure 3 DSC thermograms of nonisothermal crystallization for PA1010 (A) and PA1010/1.5 wt % nano-ZrO_2 composite coating (B) at various cooling rates.

TABLE II
Values of T_i, T_p, T_c, ΔW, and ΔH_c at Various Cooling Rates for PA1010 and PA1010/1.5 wt % Nano-ZrO_2 Composite Coating

Sample	Φ (°C/min)	T_i (°C)	T_p (°C)	$t_{1/2}$ (min)	ΔW (°C)	ΔH_c (J/g)	X_c (%)
PA1010 coating	2.5	185.3	181.7	2.23	2.5	52.49	21.51
	5	183.6	179.1	1.22	3.0	49.40	20.24
	10	181.7	176.8	0.72	4.7	48.02	19.68
	15	180.6	174.3	0.55	6.2	47.28	19.37
	20	179.7	173.0	0.47	7.8	45.24	18.54
	2.5	186.5	182.4	2.18	1.9	54.68	26.36
PA1010/n-ZrO_2	5	184.7	180.4	1.16	2.7	51.03	24.60
composite coating	10	183.0	178.1	0.7	3.5	50.68	24.43
	15	182.0	176.2	0.53	5.2	49.07	23.65
	20	181.0	174.8	0.45	6.8	46.83	23.44

(X_t), as a function of crystallization temperature (T), is defined as:

$$X_t = \frac{\int_{T_0}^{T}(dH_c/dT)dT}{\int_{T_0}^{T_\infty}(dH_c/dT)dT} \quad (2)$$

where T_0 and T_∞ represent the onset and the end of crystallization temperatures, respectively. Figure 4 summarizes the relative degree of crystallinity, X_t, versus the temperature for pure PA1010 and PA1010/nano-ZrO_2 composite coating at various cooling rates. All of these curves have the same sigmoidal shape, implying that the lag effect of the cooling rate on crystallization was observed only. The temperature parameters in Figure 4 could be converted into a timescale with the following relation:

$$t = \frac{(T_0 - T)}{\Phi} \quad (3)$$

where T is the temperature at crystallization time t, and Φ is the cooling rate. Typical plots of the relative degree of crystallinity as a function of time are illustrated in Figure 5. The time for completing the crystallization shorts with the cooling rate increasing. The half time of crystallization ($t_{1/2}$) of PA1010 and PA1010/nano-ZrO_2 composite coating can be determined from Figure 5, and the results are listed in Table II. As expected, the value of $t_{1/2}$ decreased with increasing cooling rates for both PA1010 coating and PA1010/nano-ZrO_2 composite coating. However, the value of $t_{1/2}$ for PA1010/nano-ZrO_2 composite coating was lower than that for PA1010 coating at given cooling rate, signifying that the addition of nano-ZrO_2 could accelerate the overall crystallization process.

To investigate kinetics parameters for the nonisothermal crystallization process, several methods, as follows,[16–18] based on the Avrami equation have been developed successively.

Modified Avrami equation

Based on the assumption that the crystallization temperature is constant, the Avrami equation can be directly used to describe the primary stage of non-

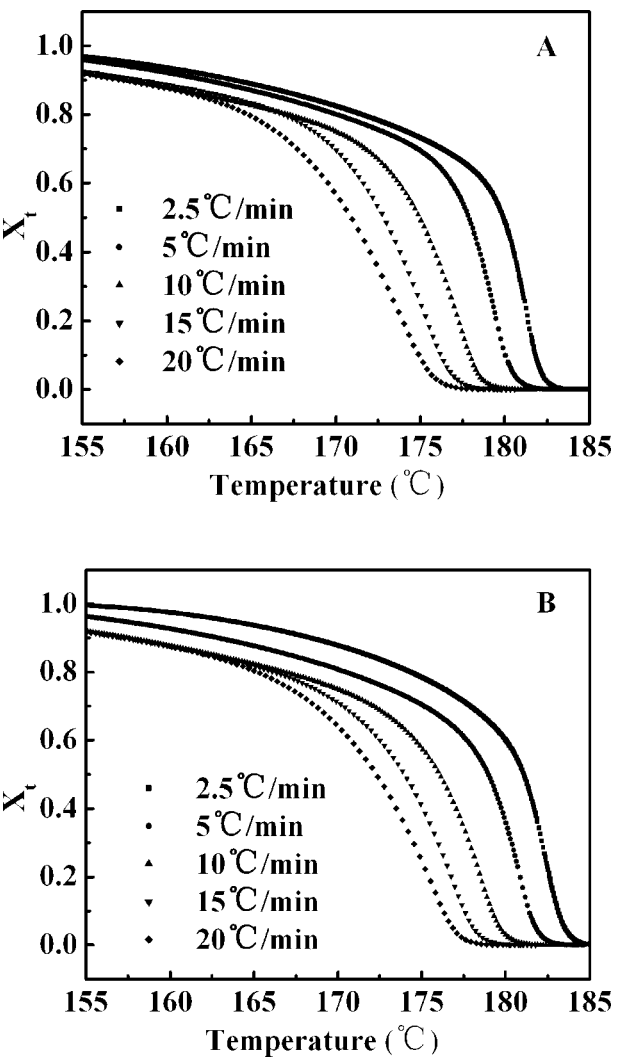

Figure 4 Plots of X_t versus T for crystallization of PA1010 coating (A) and PA1010/1.5 wt % nano-ZrO_2 composite coating (B).

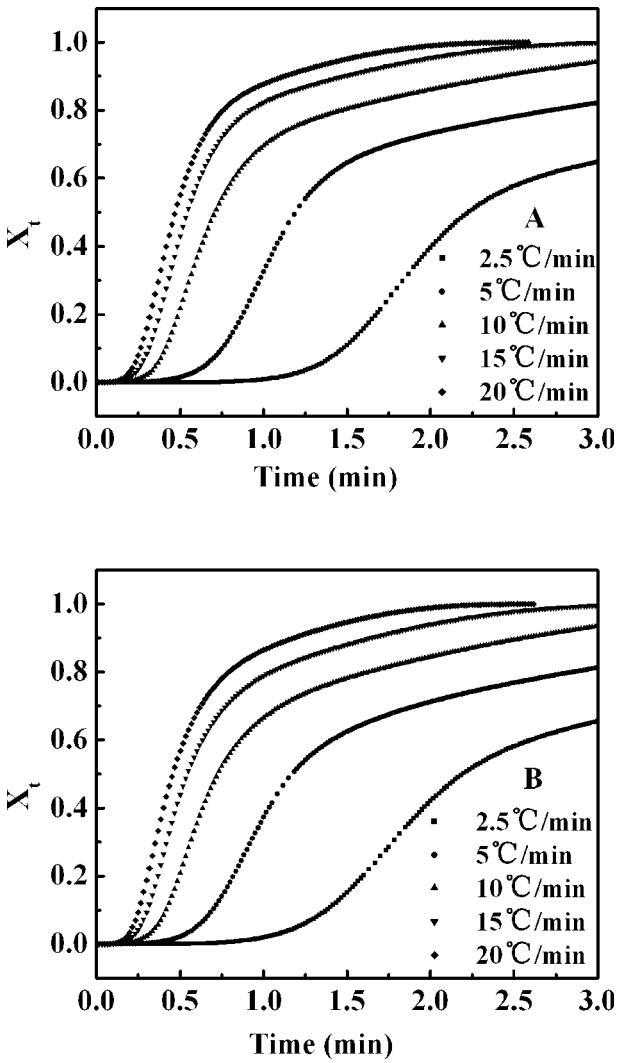

Figure 5 Plots of X_t versus time for crystallization of PA1010 coating (A) and PA1010/1.5 wt % nano-ZrO_2 composite coating (B).

isothermal crystallization. In this case, the Avrami equation is expressed as:

$$1 - X(t) = \exp(Z_t t^n) \tag{4}$$

where the exponent n is a mechanism constant depending on the type of nucleation and growth process parameters, and Z_t is a composite-rate constant involving both nucleation and growth-rate parameters. Using eq. (4) in double-logarithmic form

$$\ln[-\ln(1 - X_t)] = \ln Z_t + n \ln t \tag{5}$$

Considering the nonisothermal character of the process investigated, the value of Z_t determined from eq. (4) should be inadequate due to the influence of the cooling rate. Assuming that the cooling rate is constant or approximately constant, the final form of the parameter characterizing the kinetics of nonisothermal crystallization is given as follows:[16]

$$\ln Z_c = \frac{\ln Z_t}{\Phi} \tag{6}$$

Drawing the straight line given by eq. (5) enable one to obtain the Avrami exponent n and the rate parameter Z_t or Z_c from the slope and the intercept, respectively.

Figure 6 presents plots of $\ln[-\ln(1 - X_t)]$ versus ln t for crystallization of PA1010 coating and PA1010/nano-ZrO_2 composite coating. The values of the Avrami exponent n and the rate parameter Z_c (i.e. corrected Z_t) can be determined from the slope and intercept of the curves, respectively. Since the temperature changes constantly under nonisothermal crystallization, Z_t and n in nonisothermal crystallization do not have the same physical significance as in

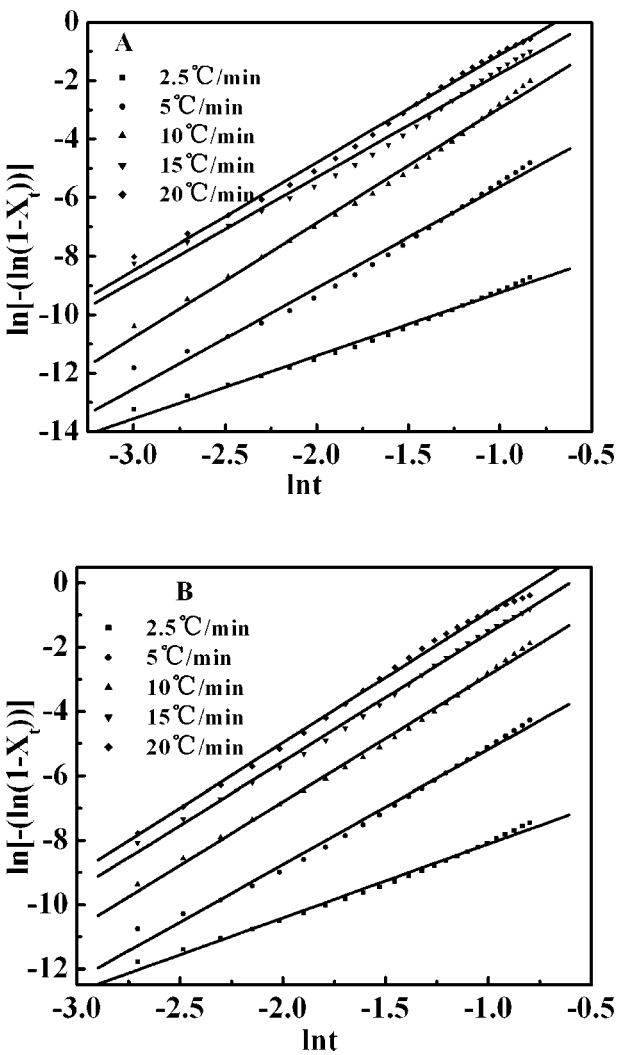

Figure 6 Plots of $\ln[-\ln(1 - X_t)]$ versus lnt for crystallization of PA1010 coating (A) and PA1010/1.5 wt % nano-ZrO_2 composite coating (B).

TABLE III
Parameters of PA1010 Coating and PA1010/1.5 wt % Nano-ZrO_2 Composite Coating During Non-Isothermal Crystallization Process

		Φ (°C/min)				
Sample	2.5	5	10	15	20	
PA1010 coating	Zc	0.06	0.650	1.10	1.13	1.14
	N	2.15	3.45	3.91	3.54	3.68
PA1010/n-ZrO_2	Z_c	0.10	0.73	1.10	1.17	1.16
composite coating	*N*	2.30	3.58	3.94	3.97	4.05

the isothermal crystallization. Consequently, it will affect the rates of both nuclei formation and spherulite growth because of the temperature dependent. In this case, Z_t and n could be considered as two adjustable parameters only to be fit to the data. Although the physical meaning of Z_t and n could not be related in a simple way to the nonisothermal case, eq. (6) provided further insight into the kinetics of nonisothermal crystallization.

The derived parameters are list in Table III. n values of the PA1010 coating vary from 2.15 to 3.68, and those of the PA1010/nano-ZrO_2 composite coating range from 2.30 to 4.05, which means the addition of the nano-ZrO_2 influences the mechanism of nucleation and the growth of PA1010 crystallites. The larger the rate parameter Z_c value, the higher the crystallization rate is. As expected, the value of Z_c increased with increasing cooling rates for both PA1010 and PA1010/nano-ZrO_2 composite coating.

Ozawa model

Ozawa[17] assumed that the nonisothermal crystallization process was composed of infinitesimally small isothermal crystallization steps and extended the Avrami equation to the nonisothermal process. Ozawa's theory can be expressed as:

$$1 - X_t = \exp\left[\frac{-K(T)}{\Phi^m}\right] \tag{7}$$

where *K(T)* is the cooling function related to the all over crystallization rate and m is the Ozawa exponent that depends on the dimension of crystal growth.

From eq. (7), it follows:

$$\ln[-\ln(1 - X_t)] = \ln K(T) - m \ln \Phi \tag{8}$$

by plotting $\ln[-\ln(1 - X_t)]$ against $\ln \Phi$, a straight line should be obtained if the Ozawa method is valid and kinetics parameter m and *K(T)* can be derived from the slope and the intercept, respectively. Ozawa plots of $\ln[-\ln(1 - X_t)]$ versus $\ln \Phi$ for crystallization of PA1010 and PA1010/nano-ZrO_2 composite coating are presented in Figure 7. Clearly no straight lines are obtained, indicating the Ozawa model could not provide an adequate description of crystallization in both PA1010 and PA1010/nano-ZrO_2 composite coating. It could be due to the crystallization process with different cooling rates at

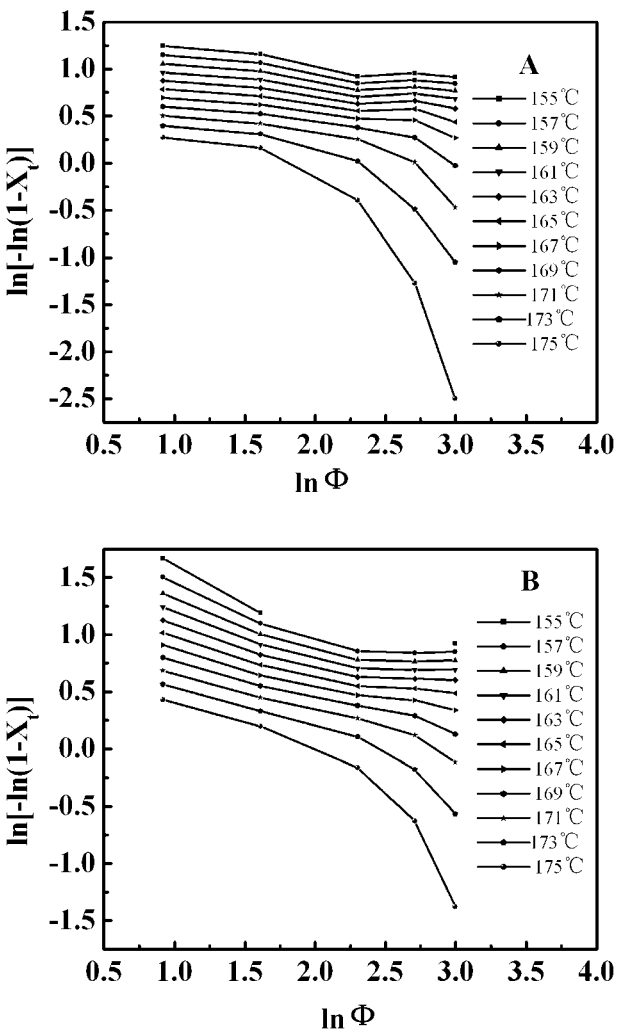

Figure 7 Ozawa plots of $\ln[-\ln(1 - X_t)]$ versus $\ln\Phi$ for crystallization of PA1010 coating (A) and PA1010/1.5 wt % nano-ZrO_2 composite coating (B).

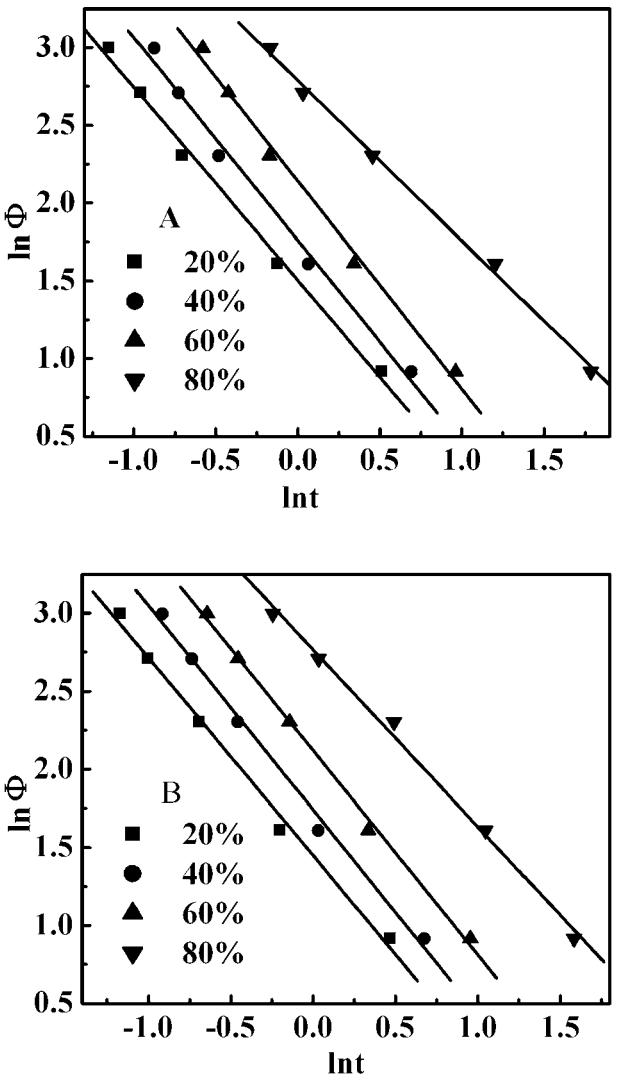

Figure 8 Plots of lnΦ versus lnt for crystallization of PA1010 coating (A) and PA1010/1.5 wt % nano-ZrO_2 composite coating (B).

various stages at a given temperature. It is the lower cooling rate process toward the end of the crystallization process. In contrast, the crystallization process is at an earlier stage at the higher cooling rate. Because nonisothermal crystallization is a dynamic process, in which the crystallization rate is no longer constant. But a function of time and cooling rate, the quasi-isothermal treatment of the Ozawa model might be questionable. In the Ozawa analysis, experimental data representing widely varying physical states of the system were compared with each other. However, these differences have not been taken into account in the model. As a result, the Ozawa exponent m is not a constant with temperature during crystallization, so that the Ozawa method cannot be applied to study the nonisothermal crystallization kinetics of PA1010 and PA1010/nano-ZrO_2 composite coating.

Combined Avrami equation and Ozawa equation

Recently, a new approach was developed by Mo and co-workers[18] to study the nonisothermal crystallization of crystalline and semi-crystallization polymers. For the nonisothermal crystallization process, physical variables relating to the process are the relative degree of crystallinity (X_t), Φ, and T. Both the Ozawa and Avrami equations give their relationship as follows:

$$\ln Z_t + n \ln t = \ln K(T) - m \ln \Phi \tag{9}$$

By a rearrangement at a certain value of X_t

$$\ln \Phi = \ln F(T) - \alpha \ln t \tag{10}$$

where $F(T) = [K(T)/Z_t]^{1/m}$ refers to the value of the cooling rate, which must be chosen within the unit of t when the measured system amounts to a certain degree of crystallinity. α is equal to n/m. According to eq. (10), at a given degree of crystallinity, plotting ln Φ versus ln t (Fig. 8) yields a liner relationship between ln Φ and ln t. The kinetic parameter F (T) and α were determined from the intercept and slope of the lines. They are listed in Table IV for PA1010 and PA1010/nano-ZrO_2 composite coating. In Table IV F (T) values increased with an increasing relative degree of crystallinity. However, the F (T) values of PA1010/nano-ZrO_2 composite coating are lower

TABLE IV
Values of F (T), a, and CRC for PA1010 and PA1010/Nano-ZrO_2 Composite Coating

Sample	X_t (%)	$F(T)$	a	CRC
PA1010 coating	20	1.50	1.24	1.99
	40	1.76	1.30	
	60	2.14	1.33	
	80	2.79	1.03	
PA1010/n-ZrO_2	20	1.45	1.27	2.23
composite coating	40	1.74	1.31	
	60	2.12	1.3	
	80	2.76	1.13	

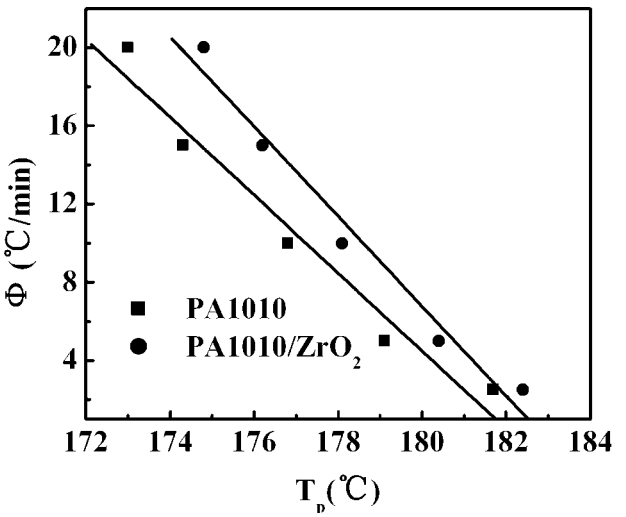

Figure 9 Plots of Φ versus T_p for PA1010 coating and PA1010/1.5 wt % nano-ZrO_2 composite coating.

than those of PA1010 coating, that is, the nanocomposite coating can reach the same crystallinity degree at higher temperature compared with pure PA1010 coating.

To compare the crystallization rate of different polymers, Khanna[19] introduced a ''crystallization rate coefficient'' (CRC), which can be obtained from the slope of Φ versus T_p in Figure 9. The higher the CRC is, the faster the crystallization is. The crystallization rate of PA1010/nano-ZrO_2 composite coating is faster than that of PA1010 from CRC listed in Table IV.

Nucleation activity

Dobreva and Gutzow[20,21] suggested a simple method for calculating the nucleation activity of foreign substrates in polymer melt. This method has been also used for silica nanoparticle-filled PEN[22] and for surface modified talc PP composites[23]. Nucleation activity (φ) is a factory by which the work of three-dimensional nucleation decreases with the addition of a foreign substrate. If the foreign substrate is extremely active, φ approaches 0, while for inert particles, φ approaches 1. The nucleation activity is calculated from the ratio:

$$\varphi = B^*/B \tag{11}$$

where B is a parameter calculated from the following equation:

$$B = \omega\delta^3 V_m^2/3nk_B T_m^0\ \Delta S_m^2 \tag{12}$$

where ω is a geometric factor, δ is a specific energy, V_m is the molar volume of the crystallizing substance, n is the Avrami exponent, ΔS_m is the entropy of melting and T_m^0 the infinite crystal melting temperature.

Furthermore, B can be experimentally determined from the slope of eq. (13) obtained by plotting ln Φ versus the inverse squared degree of supercooling $1/\Delta T^2$ ($\Delta T = T_m - T_i$)[15,16]

$$\ln\Phi = \text{Constant} - B/\Delta T^2 \tag{13}$$

The above equation holds for homogeneous nucleation from a melt, near the melting temperature. By using a nucleating agent, eq. 13 is transformed to the following for heterogeneous nucleation:

$$\ln\Phi = \text{Constant} - B^*/\Delta T^2 \tag{14}$$

Plots of ln Φ versus $1/\Delta T^2$ for the PA1010 and PA1010/nano-ZrO_2 composite coatings are shown in

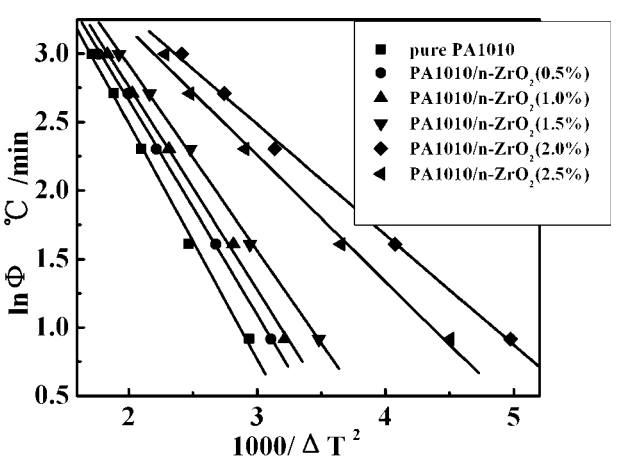

Figure 10 Plots of lnΦ versus $1/\Delta T^2$ for PA1010 coating and PA1010/nano-ZrO_2 composite coatings.

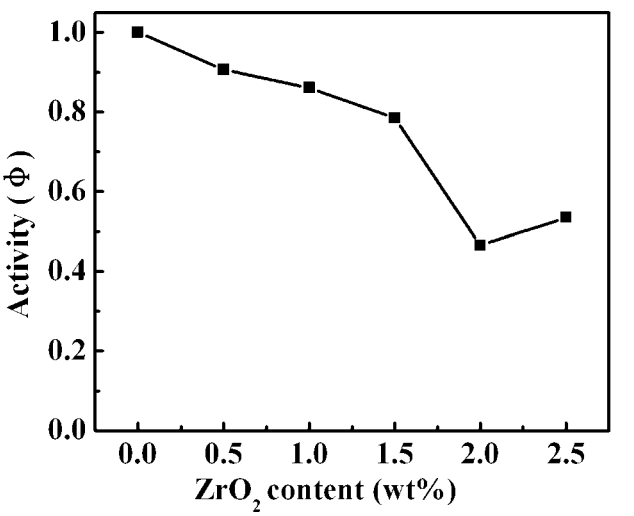

Figure 11 Variation of nucleation activity (φ) with zirconia content for the PA1010/nano-ZrO_2 composite coatings.

Figure 10. As it can be seen straight lines are obtained in every sample. From the slopes of these lines, the values of B and B^* for the PA1010 and PA1010/nano-ZrO_2 composite coating can be calculated, respectively. Then, the nucleation activity is computed from eq. (11). The effect of the amount of the nano-ZrO_2 on the activity is presented in Figure 11. All of these results reveal that the nucleation effect increased with increasing ZrO_2 content, indicating that nano-ZrO_2 was acting effectively as a nucleation agent in the PA1010. However, after a certain amount (i.e., 2.0 wt %) a plateau is observed meaning that after this amount nucleation is slightly affected.

CONCLUSION

The PA1010/nano-ZrO_2 composite coating was prepared by flame spraying in this work. For analysis the experiment process, three methods were used to investigate the nonisothermal crystallization process of PA1010/nano-ZrO_2 composite coating. Moreover, the Ozawa analysis failed to provide an adequate description of the nonisothermal crystallization of PA1010 and PA1010/nano-ZrO_2 composite coating. But the modified Avrami analysis by Jeziorny and a method developed by Mo et al. were successful for describing the nonisothermal crystallization process of this system. The half-time $t_{1/2}$ and Z_c showed that the crystallization rate of PA1010 and PA1010/nano-ZrO_2 composite coating increased with cooling rates increasing. In contrast, the crystallization rate of PA1010/nano-ZrO_2 composite coating was faster than that of PA1010 at a given cooling rate, proved the nano-ZrO_2 act as nucleation agents in the PA1010 matrix. Faster crystallization and higher crystallinity can result in the superior mechanical and friction properties of PA1010 nanocomposite coatings.

References

1. Kumar, S.; Selvarajan, V.; Padmanabhan, P. V. A.; Sreekumar, K. P. Surf Coat Tech 2006, 201, 1267.
2. Cho, J. E.; Hwang, S. Y.; Kim, K. Y. Surf Coat Tech 2006, 200, 2653.
3. Fedrizzi, L.; Rossi, S.; Cristel, R.; Bonora, P. L. Electrochim Acta 2004, 49, 2803.
4. Kim, J. H.; Yang, H.; Baik, K.; Seong, B. G.; Lee, C.; Hwang, S. Y. Curr Appl Phys 2006, 6, 1002.
5. Boudi, A. A.; Hashmi, M. S. J.; Yilbas, B. S. J Mater Pro Tech 2006, 174, 44.
6. Edrisy, A.; Perry, T.; Alpas, A. T. Wear 2005, 259, 1056.
7. Sahraoui, T.; Guessasma, S.; Fenineche, N. E.; Montavon, G.; Coddet, C. Mater Lett 2004, 58, 654.
8. Eigen, N.; Klassen, T.; Aust, E.; Bormann, R.; Gärtner, F. Mater Sci Eng A 2003, 356, 114.
9. Mo, Z. S.; Meng, Q. B.; Feng, J. H.; Zhang, H. F.; Chen, D. L. Polym Int 1993, 32, 53.
10. Lu, X. F.; Hay, J. N. Polymer 2001, 42, 9423.
11. Carvalho, B. D.; Bretas, R. E. S. J Appl Polym Sci 1999, 72, 1741.
12. Wu, T. M.; Hsu, S. F.; Chien, C. F.; Wu, J. Y. Polym Eng Sci 2004, 44, 2288.
13. Wang, B.; Sun, G. P.; Liu, J. J.; He, X. F.; Li, J. J Appl Polym Sci 2006, 100, 3794.
14. Zeng, H. L.; Gao, C.; Wang, Y. P.; Watt, P. C. P. S.; Kong, H.; Cui, X. W.; Yan, D. Y. Polymer 2006, 47, 113.
15. Li, Y.; Zhang, H.; Xie, B. Tribology 2004, 24, 429.
16. Jeziorny, A. Polymer 1978, 19, 1142.
17. Ozawa T. Polymer 1971, 12, 150.
18. Liu T. X.; Mo, Z. S.; Wang, S. G.; Zhang, H. F. Polym Eng Sci 1997, 37, 568.
19. Khanna, Y. P. Polym Eng Sci 1990, 30, 1615.
20. Dobreva, A.; Gutzow, I. J Non-Cryst Solids 1993, 162, 1.
21. Dobreva, A.; Gutzow, I. J Non-Cryst Solids 1993, 162, 13.
22. Kim, S. H.; Ahn, S. H.; Hirai, T. Polymer 2003, 44, 5625.
23. Alonso, M.; Velasco, J. I.; De Saja, J. A. Eur Polym J 1997, 33, 255.